5

COORDINATION POLYMERIZATION

João B. P. Soares and Odilia Pérez

5.1 INTRODUCTION

This chapter describes the coordination polymerization of acyclic and cyclic vinylic monomers, conjugated dienes, and polar vinylic monomers with the most important catalytic systems known in this area. A chronological classification for the development of the main coordination catalyst types is outlined, as well as polymerization kinetics and mechanisms and applications of polymers obtained through different metallic complexes.

The reaction where vinylic monomers polymerize through coordination at the metallic center of some catalytic species is called *coordination polymerization*. Although the first catalytic system based on this kind of coordination chemistry was reported by Phillips Petroleum Co., most of the literature concerning coordination polymerization refers to the Ziegler–Natta catalysts because of their versatility in controlling chemical composition distribution (CCD) and of the wider variety of monomers they can polymerize [1].

The main early advances in the knowledge and understanding of coordination polymerization were established by studying the catalyst discovered by Ziegler in the early 1950s for ethylene polymerization, and utilized by Natta for polymerization of propylene and α-olefins. The most important contribution of Natta's works consisted in developing the Ziegler catalysts that could control polymer stereoregularity. Natta separated and characterized the three polypropylene stereoisomers—isotactic, syndiotactic, and atactic, thus opening the doors to a revolution on polyolefin applications that is still seen today.

The contributions by Ziegler and Natta caused great industrial impact and large advances in research and development of polymer science and engineering, as new kinds of polymers—such as high density polyethylene (HDPE); isotactic polypropylene (iPP); ethylene, propylene, and higher α-olefin copolymers; cis- and trans-polydienes; ethylene-propylene elastomers (EPEs); and ethylene-propylene-diene monomer (EPDM) copolymers—became commercially available in the mid-1950s. For these remarkable advances, Karl Ziegler and Giulio Natta were awarded the Nobel Prize in Chemistry in 1963, and their original discoveries have been called the *Ziegler–Natta catalysts* since then.

Other kinds of coordination catalytic systems developed few years before the Ziegler–Natta catalysts were based on chromium and molybdenum oxides supported on SiO_2 Al_2O_3 and other supports. The catalysts were patented by Phillips Petroleum and Standard Oil companies of Indiana for the synthesis of polyolefins. Although Phillips catalysts were the first to produce a fraction of crystalline polypropylene, these systems were more useful for the production of polyethylene. In fact, the Phillips and the Ziegler–Natta catalysts are currently the two commercial systems that dominate the production of HDPE [2].

The discovery of Ziegler–Natta catalysts led to many industrial and academic investigations on other kinds of metallic complexes for polymerization of different monomers. Several organometallic and coordination compounds have been synthesized and probed as catalytic systems. They have been classified based on generations or groups, transition-metal type, the chemical structure, the type of activator, and their applications in polymerization processes [2]. Currently, there are different groups of initiator systems based on early and late transition metals or lanthanide complexes, which have been studied in polymerization catalysis [3].

Handbook of Polymer Synthesis, Characterization, and Processing, First Edition. Edited by Enrique Saldívar-Guerra and Eduardo Vivaldo-Lima.

First-generation Ziegler–Natta catalysts $TiCl_4/AlEt_3$ and $TiCl_3/AlEt_2Cl$ were applied for the polymerization of ethylene and propylene, respectively. Since the mid-1970s, modifications of the original Ziegler–Natta catalysts, including crystallinity, surface area, support type, and the effect of internal and external donors, led to the development of new catalyst generations with improved activity and stereoregularity, totalizing five catalyst generations for polypropylene technology [4].

Homogeneous catalytic systems based on Cp_2TiCl_2 complexes (titanocenes) activated with alkyl or alkyl chloride aluminum compounds were also investigated by Natta and Breslow in the mid-1950s; however, they showed very low activity for ethylene polymerization and were inactive for propylene polymerization [4].

In the early 1980s, Kaminsky and Sinn discovered an efficient way to activate homogeneous metallocene catalysts with methylaluminoxane (MAO). Titanocene and zirconocene complexes activated with MAO exhibited very high activity for ethylene polymerization; these early systems, however, still had low activity for propylene polymerization and formed atactic polypropylene [5]. Metallocene/MAO systems containing stereospecific ligands could be used to catalyze the polymerization of prochiral olefins (α-olefins) through the use of catalysts with well-defined active sites [6]. Later, Brintzinger [7] and Ewen [8] reported group 4 ansa-metallocenes that are useful for obtaining iPP, and they proposed for the first time the relationship between structure and symmetry of the precursor catalysts with the stereoregularity of the polymers produced.

One of the remarkable advantages of metallocene catalysts is their ability to make polyolefins with much more uniform microstructure than the Ziegler–Natta or the Phillips catalysts. Metallocene catalysts are considered to have only one type of active site (single-site catalysts) making polymer chains with the same average properties, while heterogeneous Ziegler–Natta and Phillips catalysts are multiple-site catalyst that makes polyolefins with broad, and sometimes multimodal, microstructural distributions [9].

Monocyclopentadienyl-based organometallic complexes also promote the stereoregular polymerization of higher α-olefins and styrene [9]. Ishihara first reported the use of different "half-sandwich" titanocenes activated with MAO for the production of enriched syndiotactic polystyrene [10]. Other monocyclopentadienyl-based catalysts that show stereoregular control are the constrained geometry catalysts (CGCs) [11], which contain fixed ligands, through the ansa-heteroatom bond to the metallic center. The first CGC, reported by Dow Chemical, was the *ansa*-Cp-amidoM_TX_2 used in the polymerization and copolymerization of higher α-olefins and styrene [12]. CGCs are also considered single-site catalysts. Stereoregular polymers usually show improved mechanical properties and higher melting temperatures because of their higher crystallinity.

Nonmetallocene precursors, based on early transition metals of groups 3, 4, and 5 [13], or lanthanide complexes [3] have also been reported as single-site catalytic systems useful for the polymerization of olefins or conjugated dienes [14]. Several systems containing bulky chelated diamine [15], phosphinimide [16], phenoxyimine [17], or bisphenolic ligands [18], among others, can produce very high active systems, such as 2-salicylaldimine dichloride zirconium, known as *phenoxyimine catalyst* (FI catalyst), which exhibits high activity for ethylene polymerizations when activated with MAO [17].

Other kinds of nonmetallocene complexes based on early transition metals (mainly Ti and Zr) containing dibenzyl-chelated diamido dipyrrole [19] or tetra-amido tetrapyrrole [20] ligands, as well as some amidinate, guanidinate [21], or amidopyridine [22] groups in organometallic or coordination complexes, exhibit moderate activity for olefin and diene polymerizations and some applications to living olefin polymerization [23].

Catalytic systems for diene polymerization based on lanthanide complexes mixed with aluminum compounds were reported since 1964. La, Nd, Ce, and Sm have been the most studied metals as Ziegler-Natta-type catalysts. Lanthanide-containing organic ligands such as allyl complexes were later reported for polybutadiene syntheses, and by the mid-1990s, the number of publications on lanthanide catalysts based on cyclopentadienyl ligands increased considerably [3, 24]. Lanthanidocene complexes with bridged or unbridged ligands have been studied as catalysts for nonpolar and polar olefin polymerization or copolymerization reactions [25].

On the other hand, late transition-metal catalysts using Ni, Fe, Co, or Pd showed high activity for olefin polymerizations as well as for the incorporation of functionalized monomers [26]. Owing to their higher electronic density and bulky chelated ligands, late transition-metal catalysts are more stable and more capable of polymerizing monomers with different functional groups. Branched and hyperbranched polymeric structures can also be synthesized using late transition-metal catalysts due to the chain walking mechanism [27]. These systems were developed by Brookhart and Johnson [28], Gibson [29], Grubbs [30], and others and correspond to the later advances in catalytic systems for coordination polymerization.

Definitions, chemical and physical properties, and general features of the most relevant catalyst types used in coordination polymerizations are described in Section 5.3, after the classification by type of monomers most frequently used and studied in this kind of polymerization reactions.

TABLE 5.1 Main Polymers made by Coordination Polymerization

Thermoplastics	Copolymers (Thermoplastics)	Elastomers and Plastomers
High density polyethylene (HDPE)	Ethylene-propylene copolymers	*cis*-1,4-polybutadiene
Linear low density polyethylene (LLDPE)	Styrene-ethylene copolymers	*trans*-1,4-Polyisoprene
Isotactic polypropylene (iPP)		Random ethylene-α-olefin copolymers
Syndiotactic polypropylene (sPP)		Ethylene-propylene rubber (EPR)
trans-1,4-Polyisoprene		Ethylene-propylene-diene copolymers (EPDM)
Syndiotactic polystyrene (sPS)		
Cycloolefins		

The last part of this chapter deals with coordination polymerization kinetics and mechanism, mathematical models at different scales, as well as some analyses on the supported catalyst particle breakup and growth.

5.2 POLYMER TYPES

Polymerization by coordination is one of the most versatile methods to produce a variety of polymers. Stereoregularity is one of the outstanding characteristics of the coordination polymerization that relies on the use of catalytic systems based on organometallic or coordination complexes of special structures and symmetries to make highly stereospecific polymers.

Table 5.1 shows the main families of polymers obtained by coordination polymerization (most of them commercial polymers), which were grouped according to their thermomechanical behavior, such as polymer and copolymers, thermoplastics, elastomers, and plastomers. Most of the polymers synthesized by coordination mechanisms correspond to different grades of polyolefins and polydienes, made with Ziegler–Natta or Phillips catalyst [31].

5.3 CATALYST TYPES

5.3.1 Phillips Catalyst

The Phillips-type catalyst, first reported by Hogan in the early 1950s at the Phillips Petroleum Co., is defined as chromium oxide (CrO_3) supported on activated mixtures of silica and alumina particles with a ratio Si/Al = 87 : 13. Usually, the support particles have high surface area around 600 m^2/g. After supporting, the catalyst is activated at 500–800 °C using a dry air current, where the impregnated chromium, between 1 and 5 wt%, is stabilized as Cr(VI). Hogan determined by several methods that just 0.1% of the total supported Cr were active centers, and on the basis of the water formed per CrO_3 molecules, the chromate structure prevailed, rather than dichromate, as represented in Figure 5.1 [2].

Other researchers suspected that Cr with different valence states could lead to distinct active centers; Krauss proposed that hexavalent chromium linked to a support could be reduced to the coordinative unsaturated Cr(II) when the olefin is coordinated and starts depolymerization reaction [32].

Phillips catalysts behave in the classic coordination polymerization way: the initiation step corresponds to the generation of the active species by reduction of Cr(VI) to Cr(II); the insertion of consecutive olefins to the growing chain is the propagation step, where very high molecular weights can be obtained; and β-hydride elimination is the main chain transfer mechanism. The addition of molecular hydrogen or α-olefins promotes chain termination, producing lower molecular weight polyolefins.

Different from classical coordination polymerization, Phillips catalysts do not require activation with a cocatalyst; however, alkylaluminum complexes are usually used as scavengers in the polymerization medium [33].

5.3.2 Classical Ziegler–Natta Catalysts

Ziegler–Natta catalysts have been defined as catalytic systems containing two components—generally, the initiator

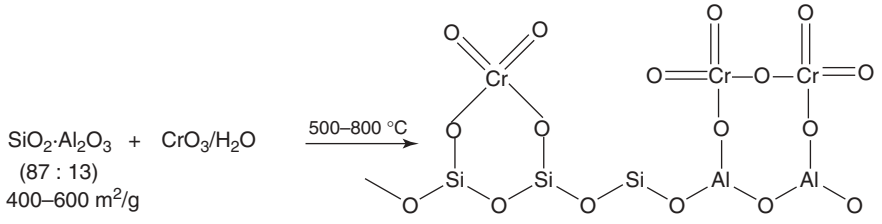

Figure 5.1 The Phillips catalyst synthesis.

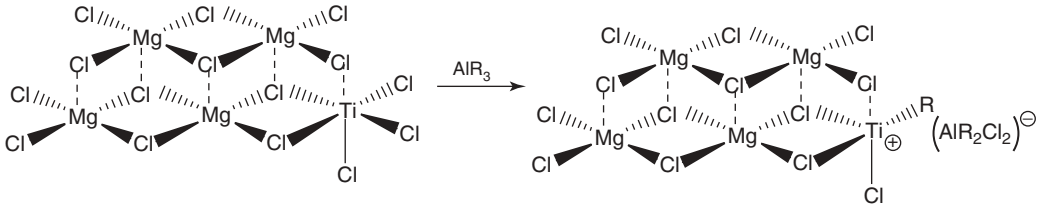

Figure 5.2 The classical Ziegler–Natta heterogenized catalyst.

or precatalyst and the component cocatalyst or activator. In the early 1950s, Ziegler determined that the mixture of metal transition halides and metallic alkyls of the main metal groups I–III (M_TCl_4 and MR_3) resulted in highly active system for the linear polymerization of ethylene. Ziegler and collaborators tried a wide variety of components using different types of transition metals, as well as metallic alkyls, determining the Ti, V, Co, and Mo, as the main transition metals potentially applied in the polymerization of different monomers. As for the cocatalysts, among the studies carried out with Al, B, Ga, Be, Mg, Li, Na, and others, the aluminum alkyls and aluminum halide-alkyls showed the best performance for the several functions carried out by the activators. Activators have three main functions in a coordination polymerization reaction: activation, stabilization, and scavenging of the polymerization medium. The activation step corresponds to the ionization of the metal by subtractions of the halide and replacement of the alkyl group in the transition metal, the conjugated base stabilizes the cationic species, and the excess of the activator works as scavenger of the polymerization medium [1].

The year following Ziegler's discovery, Natta and coworkers found that the combination of $TiCl_3$ and $AlEt_2Cl$ polymerized propylene giving a mixture of three different polymeric materials, which could be separated and characterized according to their crystallization properties. The highly crystallizable polypropylene fraction showed important physicomechanical properties such as high melting temperature, and Natta's group focused on the selective synthesis of this stereoisomer. It is important to mention again the important contribution of Natta's research group, related to the advances of stereoregularity and microstructure in the polymers obtained from propylene polymerizations or higher α-olefins, such as 1-butene, 1-hexene, and 1-octene. Natta also determined that the crystallographic structure of $TiCl_3$ was a determinant of the microstructure of the formed polypropylene. Among the allotropic crystalline structures of $TiCl_3$ (α, β, γ, and δ), the δ structure showed higher activity and better control of polypropylene stereoregularity [3, 33].

Natta also developed several techniques for the determination of the microstructure of the three stereoisomers obtained from the propylene polymerization reactions and established the terms *isotactic*, *syndiotactic*, and *atactic polypropylenes* according to the configurational position of the substituents.

After Natta found that $TiCl_3$ was the best precatalyst for propylene stereoregular polymerization and determined the importance of the physical state of the catalytic systems, his group and many other researchers strived to improve the performance of these first-generation Ziegler–Natta systems. Figure 5.2 shows the heterogenized structure of a classical Ziegler–Natta catalyst.

Currently, most of the commercial iPP is made using fourth-generation Ziegler–Natta catalysts with different internal and external donors that increase the productivity to 25 kg polypropylene/g catalyst and isotacticity from 95% to 99%. Shell Oil Co. and Montedison started commercializing these catalytic systems in the early 1980s. Shell reported the use of benzoic acid as internal and external donors, and Montedison utilized alkyl phthalates and silyl ethers as internal and external donors, respectively [3].

Polypropylene produced with these catalytic systems did not require further atactic polypropylene removal or catalyst deashing. In addition, the morphology of the polypropylene particles was considerably improved.

Recently, Basell (currently, LyondelBasell) reported the use of catalysts classified as fifth-generation Ziegler–Natta systems, through the use of Spheripol technology [34]. Very high productivities, around 100 kg polypropylene/g catalyst have been reported in this process, using 1,3-diether and succinate compounds as internal and external donors, respectively.

These techniques and synthetic methods developed for propylene by Natta and others represented the basis for the study of other stereoregular polymers, which could be obtained using the Ziegler–Natta catalysts and the more recently discovered catalytic systems. Stereospecific polymers could be made in the polymerization of other prochiral monomers such as α-olefins. The Ziegler–Natta systems also had high catalytic activity for the synthesis of polymers using dienes and could produce geometric isomers such as *cis*- or *trans*-diene polymers.

5.3.2.1 Conjugated and Non-conjugated Diene Polymerizations 1,3-Butadienes, isoprene, and 1,3-pentadiene are the conjugated diene monomers most

studied in coordination polymerization. Cyclic dienes have also been polymerized by coordination catalysts; however, the activity is lower compared to acyclic conjugated dienes, and the versatility of their isomeric structures is limited.

The first Ziegler–Natta systems used for the production of several elastomers, and crystalline polydienes, were based on Ti, Co, V, Ni, or Cr halide or nonhalide catalyst [35]. The nature of the cocatalyst is also important for the control of the stereoregularity in the polymers synthesized from dienes. AlR_3, AlR_2Cl, $AlRCl_2$, and $LiAlR_4$, where R is usually an ethyl group, have been the most used cocatalysts. The reduction and alkylating power decreases with the decrease in alkyl groups in the aluminum compounds. Although some of the catalytic systems could be similar to those used for olefin polymerizations, precatalysts containing nonhalogenated ligands showed better results for polydiene stereoregularity control, combined with the above aluminum components. Other polymerization conditions such as type of solvent, temperature, Al/M_T ratios, and crystalline structure of the M_T (Ti) are also different from that reported for olefin polymerizations. A number of articles and reviews were published by the research groups of Natta, Cooper, Marconi, and many others, and some tendencies could be related to the structure of the transition metals and the alkyl aluminum cocatalysts. It was evident that nonhalogenated cobalt based systems showed better results for the synthesis of *cis*-1,4 isomers at the expense of 1,2-units in butadiene polymerizations. For example, high *cis*-1,4-polybutadiene (99.3%) was reported by Takahasi et al. using bis(salicylaldehyde)Co(II) activated with $AlEt_2Cl$. The *trans*-1,4-polybutadiene was obtained with VCl_3, $VOCl_3$, or VCl_4 using $AlEt_3$ and $AlEt_2Cl$ as activators, and 1,2-isotactic and syndiotactic isomers were obtained with Ti and Cr catalysts, respectively. The selectivity obtained using these catalytic systems were the highest, compared to other polymerization methods, such as anionic or cationic initiation.

The physical state of the catalytic system is another parameter that could affect the behavior of the complexes, mostly related to the stereoregularity of the materials. Highly isotactic α-olefin polymers were synthesized using heterogeneous Ziegler–Natta catalysts such as $VCl_3/AlEt_3$, where VCl_3 is insoluble in hydrocarbon solvents. On the other hand, highly syndiotactic polypropylene could be obtained using soluble Ziegler–Natta catalysts such as VCl_4 and $AlEt_2Cl$ at $-78\,^{\circ}C$ [35].

After the Ziegler–Natta classical catalysts, other kind of metallic complexes were reported for the polymerization of butadienes, such as Ni-based catalysts, half-sandwich titanium complexes, or transition-metal imido compounds activated with BF_3OEt_2, $AlEt_3$, $B(C_6F_5)_4$, or MAO [3].

Recently, several lanthanide complexes, based on Nd, Ln, Sm, or Yb, have been studied for controlling stereoregularity and activity of diene polymerizations and copolymerizations. Specifically, Nd-based catalysts have shown very good stereoregularity control over the production of high *cis*-polybutadiene rubber [36].

5.3.3 Single-Site Catalysts

5.3.3.1 Metallocenes and Constrained Geometry Catalysts The introduction of organic ligands on titanium halide complexes gave rise to the obtention of new homogenous catalytic systems based on well-defined complexes, called *single-site catalysts*. Since the early 1950s, Natta and Breslow [4] (independently) studied the effect of organic ligands on Ziegler–Natta catalysts, synthesizing bis-cyclopentadienyltitanium dichloride (Cp_2TiCl_2) activated with traditional alkyl aluminum compounds, such as $AlEt_3$; however, this catalyst had very low activity for ethylene polymerization and could not polymerize propylene. Owing to its low activity, this organometallic system did not have commercial interest, but its discrete structure was useful for polymerization mechanistic studies.

Until the late 1970s and early 1980s, there was no significant progress in the catalytic activity of titanocene or zirconocene complexes, but then, Sinn and Kaminsky reported the use of MAO as an effective activator for metallocene compounds. MAO was synthesized by the controlled hydrolysis of $AlMe_3$, based on the observations of Reichert and Meyer, who by adding small amounts of water to the $Cp_2TiCl_2/AlEtCl_2$ system observed significant increase in its activity. The direct activation of group 4 metallocenes with MAO gave catalysts that were more active than the heterogeneous Ziegler–Natta complexes for ethylene polymerization and also showed high activity for propylene and higher α-olefin polymerization, but without stereoregularity control [5].

A wide variety of metallocenes containing different ligands based on indenyl (Ind) or fluorenyl (Fl) derivatives, which are isoelectronic and equivalent to cyclopentadienyl (Cp) ligands, have since been synthesized. The Cp ligands in metallocenes stabilize and control the steric environment around to the metallic center, which is the active site for olefin coordination.

In 1984, Ewen [6] and Kaminsky [5, 8], based on the study of different metallocene structures activated with MAO for the polymerization of prochiral monomers, related the symmetry of the metallocene ligands to the stereoregularity of the polymers produced. Later, Brintzinger [7] reported metallocene complexes with fixed ligands, containing interannular bridges between Cp or derivative of Cp ligands (ansa-metallocenes), giving rise to a wider variety of metallocene symmetries. Figure 5.3

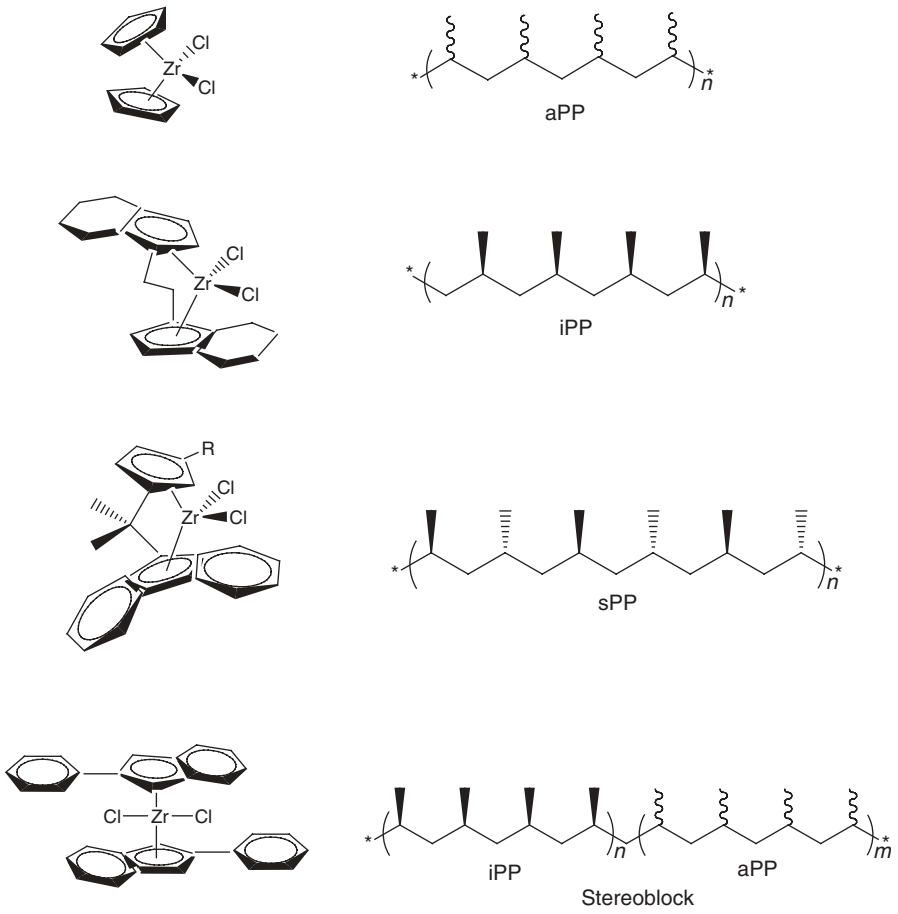

Figure 5.3 Zirconocene precursors for propylene polymerization. aPP, atactic polypropylene; sPP, syndiotactic polypropylene.

summarizes the most representative zirconocene structures, where the symmetry of the precatalysts is related to the stereoregularity of the produced polymers.

Metallocene catalysts were commercialized in 1991 by Exxon Chemical for the industrial production of ethylene-propylene (EP) elastomers in solution polymerization using zirconocene catalysts [37]. As a result of extensive research of different metallocenes applied to the stereoregular control of polymeric materials, these systems were able to produce novel polymers such as syndiotactic polystyrene and ethylene-styrene copolymers, which were not possible to produce with traditional Ziegler–Natta catalysts.

In 1985, Ishihara [10] at Indemitsu, Japan, reported that monocyclopentadienyl, indenyl, or fluorenyl titanium complexes, with different substituents on the Cp derivatives, were highly active for styrene polymerization, producing syndiotactic polystyrene with high melting temperature. Ishihara studied early transition metals from group 3 or 4; systems based on late transition metals such as Ni were inactive for styrene homo- or copolymerization. Monocyclopentadienyl complexes, also called *half-sandwich catalysts* (Fig. 5.4), were useful for styrene-ethylene copolymerizations, alternated copolymers, or block copolymers (alternated styrene-ethylene with sPS segments) when styrene is present, since it is well known that the aromatic ring helps stabilize the cationic active species through a weak coordination to the metallic center [11, 12].

Owing to its excellent physical properties, such as high melting temperature $T_m = 265–270\,^{\circ}C$ and glass-transition temperature $T_g = 100\,^{\circ}C$, besides its high resistance to solvents and chemicals, syndiotactic polystyrene is an important engineering thermoplastic utilized for different industrial applications. After the first report by Ishihara, a wide variety of monocyclopentadienyl derivative systems have been tested for styrene polymerization. Carpentier et al. [38] summarized the most relevant systems investigated for the synthesis of syndiotactic polystyrene, which are mainly based on monocyclopentadienyl Ti complexes. Different kinds of substituted indenyl, fluorenyl, and monocyclopentadienyl ligands, or dinuclear Ti half-sandwich complexes, have been reported, as well as amidinate,

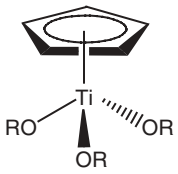

Ishihara's catalyst

Figure 5.4 Monocyclopentadienyl complex used for styrene polymerizations.

bis-phenolate, or titanatrane derivatives with different ancillary ligands, and the order of activity was reported as benzimidinate < titanatrane < half-sandwich complexes < bis-indenyl < bis-phenolate [39]. Ancillary ligands' effect was also reported, observing the highest activities and stereoregularity for complexes containing OiPr ligands.

Other kinds of monocyclopentadienyl catalysts, containing fixed Cp ligands, correspond to a*nsa*-monocyclopentadienyl group 4 complexes. Owing to their geometry, they have been called the *constrained geometry catalysts* [40]. CGCs have been active for different kinds of monomers, but the highest performance has been observed in the polymerization and copolymerization of olefins and α-olefins. The less-hindered geometry (or more open structure) at the metallic center is given by the bridged substituent from the ligand that pulls back the substituents, giving easier access to the coordination of bulkier monomers, such as styrene (Fig. 5.5).

CGCs are able to polymerize prochiral monomers, producing stereoregular polymers. Among the group 4 transition metals, titanium has shown higher activities, compared to Zr or Hf analogous systems. CGCs can make ethylene-styrene copolymers, long-chain branched (LCB) polyolefins, and polyethylene with a wide range of densities. Currently, CGCs are used in industries for producing styrene-ethylene copolymers and polyethylene resins of several densities, but it was the first catalytic system commercialized by Dow in 1991 for producing elastomers based on EP copolymers and EPDM [11].

CGCs have also been obtained with other isoelectronic Cp ligands, such as indenyl with several substituents, where the effect of the structures on the stereoregularity control of the polymers produced have been studied [40].

Other active single-site early transition-metal-based catalysts for nonpolar monomers correspond to different bis-cyclopentadienyl group 3 and lanthanide complexes, such as L_2MR (M = Sc, Y, La, Nd, Sm, Lu; R = alkyl or H). Usually, these systems do not require the activator component to generate high activity catalysts for olefin polymerizations [3].

5.3.3.2 Non-metallocene Early Transition-Metal-Based Single-Site Catalysts Intense research about new highly active catalysts for ethylene polymerization and copolymerization led to the development of new postmetallocene systems [26]. Usually, non-metallocene-based catalysts are coordination or organometallic compounds that contain bidentate or multidentate ligands such as imine, diamine, tetramine, bisphenolic, or *ortho*-phenoxyimine groups, stabilized with different bulky substituents. These systems usually are tetra-coordinated complexes, but also can be hexacoordinated, with octahedral geometry, where two or more donor groups containing nitrogen, oxygen, or phosphorus atoms form highly stable bonds with the transition metal (Fig. 5.6). Combined with the appropriate activators, nonmetallocene catalysts can promote olefin polymerization with activities comparable to those of group 4 metallocene catalysts, showing, in some cases, even higher activities.

Among the different postmetallocene catalysts in Figure 5.6, the complexes bearing phenoxyimine [17] ligands (FI catalysts) exhibit the highest ethylene polymerization activity. FI catalysts were developed by Fujita and coworkers [41] at Mitsui Chemicals, Japan, in the late 1990s.

Subsequent research accomplished by Mulhaupt [42], Cavallo [43], and others afforded the production of a wide

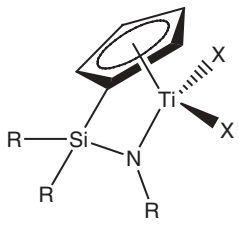

Dow's insite catalyst

Figure 5.5 Constrained geometry catalyst (CGC).

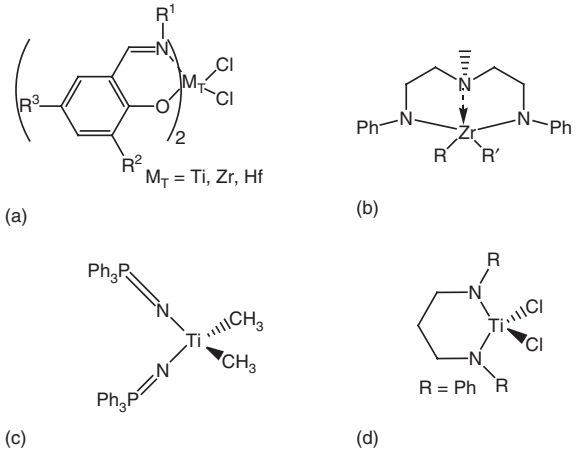

Figure 5.6 Postmetallocenes' catalytic systems: (a) phenoxyimine (FI), (b) Schrock, (c) Stephan, (d) McConville.

range of polyolefins that could not be synthesized with metallocenes efficiently. Steric and electronic effects of a variety of substituents on the phenoxyimine ligands allow these systems to produce a wide assortment of stereoregular and stereospecific polymers and copolymers, such as new differentiated polyolefins, high performance linear low density polyethylene (LLDPE), polyolefinic elastomers, cyclic olefinic copolymers, ethylene-styrene copolymers, highly isotactic and syndiotactic polypropylenes, and highly syndiotactic polystyrene, and, more recently, FI catalysts have been able to synthesize hyperbranched polyethylene [17], ethylene-polar monomer copolymers [43, 44], monodisperse poly(higher α-olefins) [18], or higher α-olefin-based block copolymers [28, 45], which are difficult to produce using the classical group 4 metallocenes or CGCs.

DFT (Density Functional Theory) calculations performed on metallocene and FI catalyst structures suggested that ethylene polymerizations involve higher energy states for metallocenes in the process of ligands exchanging, during the insertion step, than the energy states observed for FI catalysts [17]. Later, Koji and Terunor [44] postulated that the high activity of the FI complexes is based on their higher capacity for moving electronic density from the coordinating olefin, insertion and migration of the bonds and usually in all the electronic arrangement.

5.3.3.3 Late Transition-Metal Catalysts Late transition-metal catalysts typically produce branched polyethylene from polymerizing ethylene as a sole monomer, without the addition of comonomers via the mechanism of chain walking. Among the different catalytic species studied by coordination polymerization, cationic or neutral nonmetallocene complexes containing mainly Fe, Co, Ni, and Pd exhibited different ethylene polymerization behavior and single-site polymerization mechanisms (Fig. 5.7) [26]. Owing to the larger number of valence electrons, late transition-metal-based catalysts are less sensitive to protic impurities, poisons, and even polar monomers compared to catalysts based on early transition metals, such as group 4 metallocenes.

In 1981, Keim and Peuckert [45] synthesized the first branched polyethylene using iminophosphonamide-nickel complexes. The systems produced low molecular weight polyethylene with physical properties similar to LDPE. Traditionally, this kind of catalytic species is prone to facile chain transfer reactions, useful for producing ethylene dimers and oligomeric materials.

More recently, Brookhart and Johnson [28] and Gibson et al. [29] modified the structure of late transition-metal catalysts (Fig. 5.7) by introducing tridentate and bulky substituents in the ligands, thus retarding the chain termination processes in the polymerizations.

These postmetallocene single-site catalysts [46, 47] are highly active for the synthesis of branched and hyperbranched polyethylene, polypropylene, and ethylene copolymers with different α-olefins. Branching frequency and length can be controlled by varying ligand structure, temperature, and pressure during polymerization. Formation of short-chain branches during ethylene homopolymerization occurs via the chain walking mechanism, with the competition between isomerization of the chain end and the insertion for the linear growth of the polymeric chain.

Late transition-metal complexes can also polymerize nonpolar and polar comonomers, such as alkyl acrylates, acrylonitrile, or carbon monoxide. Polyketones have been efficiently produced through CO-ethylene copolymerizations [46].

Palladium/phosphine-sulfonate neutral complexes, reported by Drent, Pugh, and coworkers, could incorporate several polar comonomers such as methyl acrylate, vinyl ethers, methyl vinyl ketones, and silyl vinyl ethers. Other common comonomers such as vinyl acetate, acrylonitrile, and vinyl chloride showed very low comonomer incorporation, between 1% and 2% [48].

5.3.3.4 Supported Single-Site Catalysts Catalysts supporting is considered a prerequisite for the application of most coordination catalytic systems. The most important polymerization methods (slurry and gas phase) require the use of supported or heterogenized catalysts. Particle morphology and bulk density are the main physical features of a supported catalytic system, determining its application in commercial processes [49].

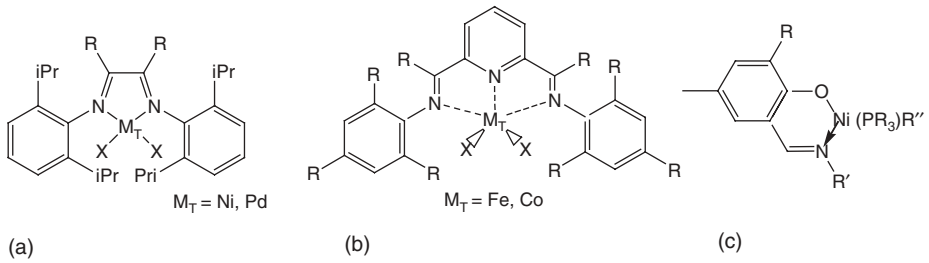

Figure 5.7 Main late transition-metal catalysts: (a) Versipol catalyst, (b) Brookhart/Gibson, (c) Grubbs/Johnson.

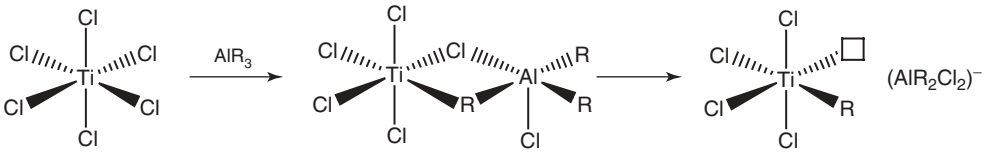

Figure 5.8 Active species formation in a classical Ziegler–Natta catalyst.

Single-site catalysts have been successfully supported on silica previously modified with MAO or trimethylaluminum, avoiding the direct contact with the Si-O or Si-OH groups of the silica support, but many other supporting techniques have been investigated. Ribeiro et al. [50] described in detail the main immobilization methods used for metallocenes, which have been extended with some modifications for other single-site catalysts. More recently, Choi and Soares have reviewed the main supporting techniques used for metallocene and postmetallocene catalysts.

5.4 COORDINATION POLYMERIZATION MECHANISM

Because of the nature of the active species, coordination polymerization has been classified as ionic polymerization, which follows the polyaddition mechanism's characteristic steps, in the growing of the polymeric chain: initiation, propagation, and termination. As for the initiation step, the ionic active species is produced by the reaction between the catalyst and cocatalyst. Usually, the catalysts are actually precursor catalysts or precatalysts, which become the real cationic active species after the activation or reaction with the cocatalyst (Fig. 5.8).

Figure 5.9 outlines the steps for the chain polyaddition mechanism involved in the coordination polymerizations for any kind of active species initiated through different cocatalysts. The counteranion species was suppressed for practical representation of the active site. Once the cationic species is created, it starts the growth of the polymeric chain through continuous addition of monomer. The propagation step is forward described in Figure 5.9 according to the most accepted reaction cycle proposed by Cossee and Arlman, which is known as the *Cossee–Arlman mechanism* [51].

As for the termination step, different reactions have been detected, according to the structure of the polymers, such as terminal vinylic groups, which are evidence of β-hydride elimination from the polymeric chains.

5.5 POLYMERIZATION KINETICS AND MATHEMATICAL MODELING

Mathematical models for olefin polymerization with coordination catalysts are usually classified into microscale, mesoscale, and macroscale models [52]. Polymerization kinetics and microstructural models are defined at the microscale level, mesoscale phenomena includes catalyst particle breakup and growth and particle mass and heat transfer resistances during polymerization, and finally, transport phenomena at the reactor level are treated in macroscale models.

This division is very useful during model development and implementation. Differentiated emphasis should be placed on these modeling scales depending on the model objectives. For instance, detailed polymerization kinetics is important if the precise prediction of polyolefin microstructure is required. On the other hand, apparent kinetics suffices if the model's objective is to follow the evolution of particle fragmentation or to describe reactor residence time effects on polymerization. These ideas are detailed in the following sections.

5.5.1 Polymer Microstructural Models

Polyethylene microstructure is defined by its distributions of chain length (CLD) or molecular weight (MWD), chemical composition (CCD), comonomer sequence length (CSLD), and LCB. In addition, polypropylene microstructure is further characterized by its distribution of regio- and stereoregularity [53, 54].

Polymer chain microstructure depends on polymerization mechanism and reactor conditions. The polymerization

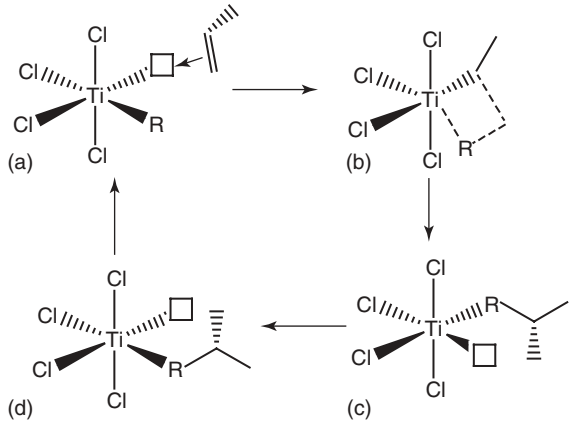

Figure 5.9 The Cossee–Arlman mechanism a) Olefin coordination, b) Olefin concerted insertion, c) Insertion step, d) Chain migration.

mechanism with coordination catalysts has been investigated extensively and is reviewed only briefly herein [39]. During polymerization, either of the two events may happen: the chain may propagate by insertion of a monomer molecule in the carbon-transition-metal bond at the end of the chain or it may terminate following several chain transfer steps. Propagation may take place with one of several comonomers or, more rarely, with a dead polymer chain having a terminal reactive double bond (macromonomer) [55]. Highly sophisticated mathematical models have been developed based on these few mechanistic steps.

Table 5.2 lists the basic kinetics steps for the homopolymerization of olefins with coordination catalysts. There are four main types of reactions: catalyst activation, monomer propagation, chain transfer, and catalyst poisoning. The reaction of the catalyst precursor, C, with the cocatalyst, Al (generally an alkylaluminum or alkylaluminoxane compound), is considered to be almost instantaneous and leads to the formation of the active catalyst site, C*. Initiation and propagation steps with monomer, M, leads to the formation of a growing polymer chain of length r, P_r. The four most common chain transfer steps are listed in Table 5.2; they produce active sites[1] that are available to grow other polymer chains and dead polymer chains of length r, D_r. Finally, the catalyst may be deactivated via first- or second-order processes or by reaction with impurities, although the details of these mechanistic steps are still poorly understood.

This kinetic model is extended to binary copolymerization of monomer types M_1 and M_2 (e.g., ethylene and 1-hexene) in Table 5.3. Not all steps from Table 5.2 are repeated in Table 5.3 to avoid unnecessary repetition, but they can be easily deduced by analogy. For copolymerizations that follow the terminal model shown in Table 5.3, the last monomer added to the living chains influences the subsequent reactions due to steric and electronic effects. For instance, four propagation steps are needed in copolymerization, since the last monomer molecule added to the chain is assumed to influence the next propagation step with monomer M_1 or M_2. Despite its apparent complexity, copolymerization models can be rendered as simple as homopolymerization ones using the pseudoconstant model developed by Hamielec and coworkers [56–59].

The kinetic steps shown in Tables 5.2 and 5.3 are widely accepted and are commonly used to develop polyolefin microstructural models, but they do not describe all aspects of olefin polymerization with coordination catalysts: (i) hydrogen not only acts as a chain transfer agent but also accelerates the polymerization rate of propylene *and* reduces the polymerization rate of ethylene with most Ziegler–Natta catalysts and metallocenes [60–65]; (ii) α-olefin accelerates the rate of ethylene polymerization significantly with most coordination catalysts, the so-called comonomer effect [61, 66, 67]; and (iii) the rate of polymerization with respect to monomer concentration may vary from 1 to 2 [68]. Several alternative hypotheses have been proposed to explain these phenomena, but there is no unified mechanism that can account for all of them.

TABLE 5.2 Basic Mechanism for Olefin Homopolymerization with Coordination Catalysts

Description	Chemical Equations
Site activation	$C + Al \rightarrow C^*$
Initiation	$C^* + M \rightarrow P_1$
Propagation	$P_r + M \rightarrow P_{r+1}$
β-Hydride elimination	$P_r \rightarrow C^* + D_r$
Transfer to H_2	$P_r + H_2 \rightarrow C^* + D_r$
Transfer to monomer	$P_r + M \rightarrow C^* + D_r$
Transfer to cocatalyst	$P_r + Al \rightarrow C^* + D_r$
First-order deactivation	$P_r \rightarrow C_d + D_r$
	$C^* \rightarrow C_d$
Second-order deactivation	$2P_r \rightarrow 2C_d + 2D_r$
	$2C^* \rightarrow 2C_d$
Poisoning	$P_r + I \rightarrow C_d + D_r$
	$C^* + I \rightarrow C_d$

Abbreviations: C, catalyst precursor; C*, active site; C_d, deactivated site; Al, cocatalyst; M, monomer; P_r, living chain of length r, D_r, dead chain of length r; H_2, hydrogen; I, catalyst poison.

[1]Active sites produced after different chain transfer steps may differ slightly. For instance, a metal hydride site is obtained after chain transfer to hydrogen, while a metal-C_2H_5 site is obtained after chain transfer to polymer. For the sake of simplicity, these sites are not differentiated in Table 5.2; for most modeling applications, these differences are also irrelevant.

TABLE 5.3 Simplified Terminal Model for Binary Copolymerization of Olefins

Description	Chemical Equations
Initiation	$C^* + M_1 \rightarrow P_1^1$
	$C^* + M_2 \rightarrow P_1^2$
Propagation	$P_r^1 + M_1 \rightarrow P_{r+1}^1$
	$P_r^1 + M_2 \rightarrow P_{r+1}^2$
	$P_r^2 + M_1 \rightarrow P_{r+1}^1$
	$P_r^2 + M_2 \rightarrow P_{r+1}^2$
β-Hydride elimination	$P_r^1 \rightarrow C^* + D_r$
	$P_r^2 \rightarrow C^* + D_r$
Transfer to hydrogen	$P_r^1 + H_2 \rightarrow C^* + D_r$
	$P_r^2 + H_2 \rightarrow C^* + D_r$
Monomolecular deactivation	$P_r^1 \rightarrow C_d + D_r$
	$P_r^2 \rightarrow C_d + D_r$

M_1 and M_2, monomer types.
Superscripts 1 and 2 indicate the type of last monomer added to the chain.

The method of moments is one of the oldest techniques used to model the MWD of polyolefins [69]. First, it is necessary to develop population balances for living and dead chains (P_r and D_r) of all lengths using the mechanisms proposed in Table 5.2 or 5.3. For high polymers, this procedure generates a very large system of ordinary differential equations (ODEs), with one equation for each chain having from 1 to r_{max} monomer units, where r_{max} is the number of monomer molecules in the longest chain in the polymer population. Solving the resulting set of ODEs requires sophisticated algorithms and considerable computational effort. If the whole distribution is not required, moment equations can be derived from the ODE system, resulting in a much smaller set of ODEs. For instance, the number-average chain length (r_n) is calculated as the ratio of the first to the zeroth moment; the weight-average chain length (r_w), as the ratio of the second to the first moment; higher chain length averages are found in a similar way. The method of moments not only reduces the required computational effort significantly but also results in a considerable loss of information since only averages are computed instead of the complete CLD. Tutorial-style descriptions of this method have been published recently in the literature [53, 54].

Alternatively, the complete population balance can be solved dynamically using efficient ODE solvers [70, 71]. The versatile commercial software PREDICI can solve population balances that describe polymerizations with coordination catalysts and many other polymerization mechanisms [72]. In this approach, the complete microstructural distributions are modeled, leading to a detailed description of the polymer microstructure.

In some specific cases, analytical solutions for the population balances can also be derived. For instance, Soares and Hamielec [73, 74] obtained analytical dynamic solutions to describe how the CLD of polyolefins varied as a function of time in stopped-flow reactors commonly used for mechanistic studies on olefin polymerization kinetics and mechanism [75–78]. These analytical solutions combine the power of full population balance numerical solutions with the ease and convenience of using closed form equations; they are, unfortunately, difficult to attain for more complex cases.

Different from analytical dynamic solutions, *instantaneous distributions* are derived to describe the polymer microstructure made at a particular instant in time during the polymerization. These distributions are "snapshots" of the polymer microstructure at a given moment during the polymerization. A classic instantaneous distribution used to describe the CLD of linear polyolefins and other polymers that follow analogous chain growth kinetics was developed independently by Schulz [79] and Flory [80, 81]

$$w(r) = r\tau^2 e^{-r\tau} \tag{5.1}$$

where $w(r)$ is the weight CLD, r is the polymer chain length, and the parameter τ is the reciprocal of the number-average chain length for the polymer. Therefore, τ is also given by the ratio of overall chain transfer, R_t, to propagation, R_p,

$$\tau = \frac{R_t}{R_p} \tag{5.2}$$

Using the mechanism proposed in Table 5.2, Equation 5.2 becomes

$$\tau = \frac{k_{tM}}{k_p} + \frac{k_{t\beta} + k_{tH}[H_2] + k_{tAl}[Al]}{k_p[M]} \tag{5.3}$$

where k_p, k_{tM}, $k_{t\beta}$, k_{tH}, and k_{tAl} are the rate constants for propagation, transfer to monomer, β-hydride elimination, transfer to hydrogen, and transfer to cocatalyst, respectively.

Equation 5.1 is applicable to polyolefins made with single-site catalysts, such as metallocenes, and predicts a polydispersity index of 2.0. It is discussed later how this equation can also be used to model the CLD of polyolefins made with multiple-site catalysts, such as heterogeneous Ziegler–Natta and Phillips catalysts. Despite its simplicity, this equation can be used to predict the complete CLD of single-site polyolefins instantaneously using an easy-to-estimate parameter, τ.

Stockmayer [82] extended the Flory distribution to also include the CCD of linear polyolefins,

$$w(r, y) = r\tau^2 e^{-r\tau} \sqrt{\frac{r}{2\pi\beta}} e^{-\frac{ry^2}{2\beta}} \tag{5.4}$$

where y is the difference between the molar fraction of monomer 1 (e.g., ethylene) in the copolymer chain, F_1, and the *average* molar fraction of monomer 1 in the whole copolymer sample, $\bar{F}_1$,

$$y = F_1 - \overline{F_1} \tag{5.5}$$

and the parameter β is defined as

$$\beta = \overline{F_1}\left(1 - \overline{F_1}\right)\sqrt{1 - 4\overline{F_1}\left(1 - \overline{F_1}\right)\left(1 - r_1 r_2\right)} \tag{5.6}$$

where r_1 and r_2 are the reactivity ratios. The variable r and the parameter τ have the same meaning as in the Flory most probable distribution (Eq. 5.1). The average molar fraction of comonomer 1 in the copolymer, $\bar{F}_1$, is calculated with the classical Mayo–Lewis equation [83]. The Stockmayer distribution is illustrated in Figure 5.10 for a single-site catalyst.

The Stockmayer distribution is an extension of the Flory distribution for copolymers. When Equation 5.4 is integrated over all chemical compositions, it is reduced to

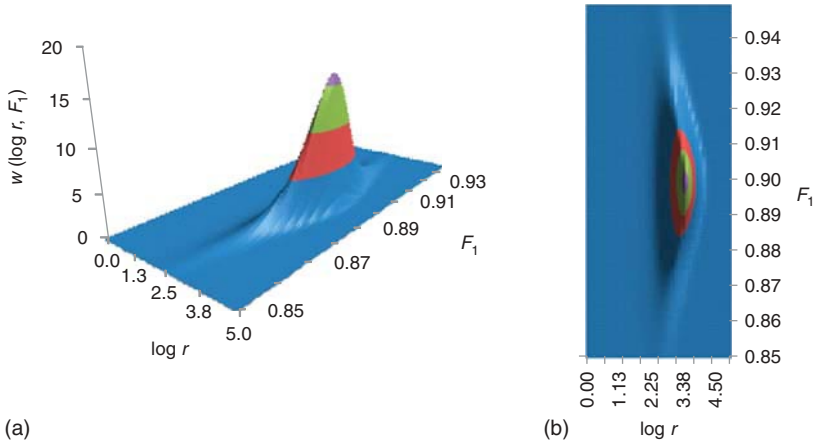

Figure 5.10 The Stockmayer distribution for a copolymer made with a single-site catalyst. a) Three-dimensional plot, b) Bird's eye view. (*See insert for the color representation of the figure*.)

the Flory distribution; similarly, when it is integrated over all chain lengths, the CCD component is isolated [84–86].

CSLD is another important microstructural characteristic of polyolefins. It is usually expressed by their dyad, triad, tetrads, and higher "ad" distributions, as measured by ^{13}C NMR. CSLD is described with Markovian statistical models [87, 88]. The order of a Markovian model indicates the number of monomer units in the growing chain that affect the propagation of the next monomer molecule. For a given catalyst, zeroth-order models assume that monomer propagation depends only on the type of monomer being inserted and not on the chain end type—these models are also called *Bernoullian models*. First-order models assume that propagation depends on the type of monomer being inserted *and* on the type of monomer at the chain end bonded to the active site—this is the terminal model discussed in Table 5.3 and also assumed in the Mayo–Lewis equation. Second-order models suppose that the type of propagating monomer and the last two monomers added to the chain influence propagation (penultimate model). Higher Markovian models follow an analogous rationale. For olefin polymerization, the terminal model is generally enough to describe the CSLD of most polyolefins, with the penultimate model being used much more rarely. A similar approach may also be used to model stereo- and regiosequences for polypropylene.

Soares and Hamielec extended the Stockmayer distribution for copolymers containing LCBs, where the mechanism of LCB formation is terminal branching via macromonomer incorporation [89, 90]. The resulting trivariate distribution is given by the expression

$$w(r, y, k) = \frac{1}{(2k+1)!} r^{2k+1} \tau_B^{2k+2} e^{-r\tau_B} \sqrt{\frac{r}{2\pi\beta}} e^{-\frac{ry^2}{2\beta}} \quad (5.7)$$

where k is the number of LCBs per chain and the parameter τ_B is a modification of the parameter τ given in Equation 5.2 to account for the rate of LCB formation, R_{LCB},

$$\tau_B = \tau + \frac{R_{LCB}}{R_p} \quad (5.8)$$

Figure 5.11 illustrates how the CLD and CCD vary for polymer populations with different number of LCBs per chain. Several other related distributions have been developed to describe these branched homopolymers and copolymers [55].

Polymer reactor dynamics involves changes in polymerization temperature, monomer/hydrogen ratio, monomer/comonomer ratio, etc. Most olefin polymerization reactors are operated under steady-state conditions; therefore, these changes are important only during grade transitions or process instabilities. They are generally very slow compared to the chain growth and termination dynamics that determine the polymer microstructures described with the instantaneous distributions mentioned earlier. Consequently, except in special cases, these distributions can be integrated in time to describe the microstructure of polymers made during non-steady-state conditions. For instance, the cumulative CLD of a polyolefin made in the time interval Δt at transient conditions, $\bar{w}(r)$, can be calculated with the equation

$$\bar{w}(r) = \frac{\int_t^{t+\Delta t} w(r, t) R_p(t) dt}{\int_t^{t+\Delta t} R_p(t) dt} \quad (5.9)$$

Since the reactor conditions are not at steady state, the instantaneous distribution $w(r, t)$ becomes a function of time. For instance, changes in hydrogen/ethylene

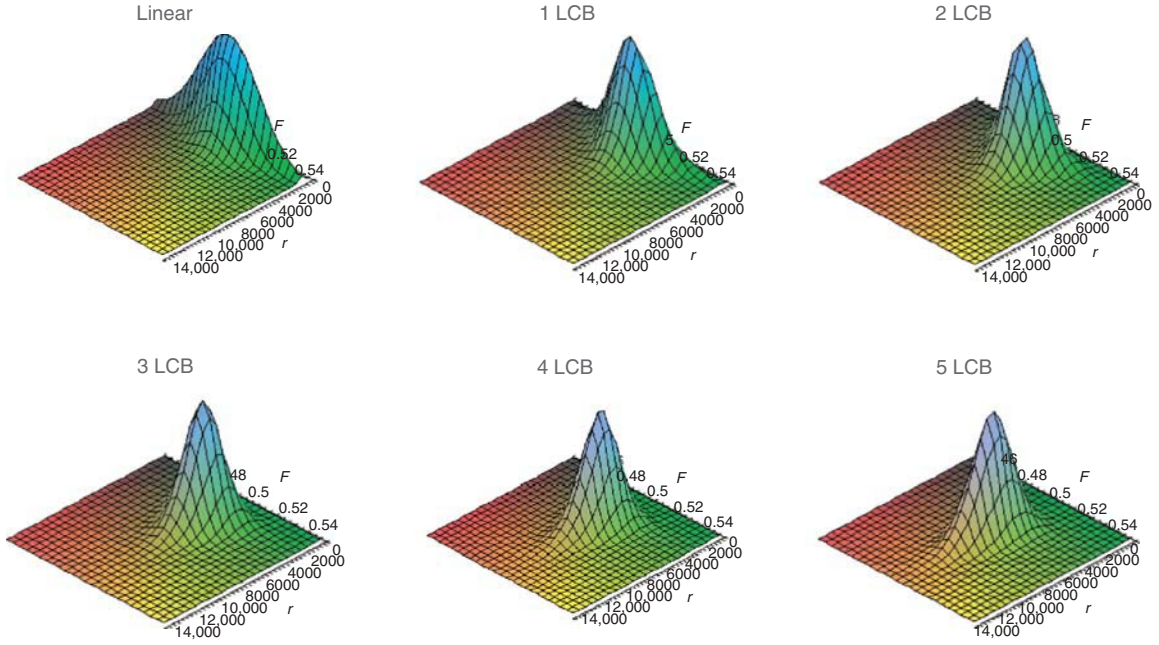

Figure 5.11 Trivariate distribution for a model polymer. (*See insert for the color representation of the figure*.)

ratio during a grade transition will make the molecular weight averages drift from one steady-state value to another.

Analogous equations can be used with any other instantaneous distribution. This relatively easy integration extends the use of instantaneous distributions to transient reactor operation and considerably broadens the use of this powerful technique. When compared with the method of moments, instantaneous distribution allows for the complete prediction of CLD and CCD instead of only averages; when contrasted to the full solution of the population balances, the method of instantaneous distributions provides the same information at a much shorter time using a more elegant solution, allows the modeler to analyze the problem with a simple glance at the equation, and can even be implemented on simple commercial spreadsheets for easy calculation.

The Monte Carlo techniques are the most powerful of all modeling approaches used to describe the microstructure of polyolefins, because chains are built individually and, in principle, *all* microstructural details can be retrieved at the end of the simulation. The main concept behind the Monte Carlo simulation is relatively simple, although model implementation and algorithm development may become sophisticated to enhance computational efficiency. One starts by defining model probabilities based on the polymerization mechanism and then uses a random number generator to decide which event should take place during polymerization. In the simplest of all cases, one can start by assuming that only two events take place during polymerization: propagation and chain transfer. This leads to the definition of a propagation probability, P_p, and a termination probability, P_t,

$$P_p = \frac{R_p}{R_p + R_t} \tag{5.10}$$

$$P_t = \frac{R_t}{R_p + R_t} = 1 - P_p \tag{5.11}$$

These two probabilities are used to build chains, one by one, during the simulation. A random number is generated between 0 and 1 and its value is compared to P_p (or P_t). If the random number is lower than P_p, the chain grows by one monomer unit; otherwise, it terminates. The CLD can be obtained through this approach after the generation of a sufficiently large number of polymer chains; generally, several hundred thousand chains are required to obtain a smooth distribution.

It is evident that this approach is impractical for this simple problem because the Flory distribution provides the same information in a much more efficient way. The Monte Carlo methods become more attractive when modeling complex microstructures for which no analytical solutions are possible, such as for terpolymers, branched or crosslinked chains, and chains with branching resulting from chain walking with late transition-metal catalysts. The Monte Carlo techniques have been used to model a variety of polyolefin microstructures effectively and are the most powerful, albeit the most computational time consuming, of all modeling techniques [91–96].

The simple approach discussed above is valid for steady-state Monte Carlo simulations, but dynamic simulations are also possible. In this case, the model probabilities must be updated frequently, generally after every iteration. A detailed discussion of these methods would be too lengthy to be included herein; the most common algorithm for dynamic Monte Carlo simulation follows the approach proposed by Gillespie, which requires the discretization of the polymerization reactor with small control volumes and the conversion of the polymerization kinetic rates into molecular collision frequencies [97, 98].

The methods discussed above for single-site catalysts (metallocenes and late transition-metal catalysts) can be extended directly to multiple-site catalysts (Ziegler–Natta and Phillips catalysts) by assuming that each site type behaves essentially as single-site catalysts [87, 88, 99, 100, 101]. Therefore, the microstructural distribution of a polymer made with a multiple-site catalyst is treated as a weighted sum of several single-type distributions [102],

$$w(r, y) = \sum_{j=1}^{n} m_j w(r, y)_j \tag{5.12}$$

where m_j is the mass fraction of polymer made on site type j for a catalyst having n site types. The simulated bivariate distribution of a polymer made on a three-site-type catalyst is shown in Figure 5.12.

This approach has been used by several researchers to model the microstructures of polymers made with the Ziegler–Natta and the Phillips catalysts using the method of instantaneous distributions, method of moments, or the Monte Carlo simulation. Several techniques have also been developed to help estimate model parameters for these multiple-site models, but it still remains a difficult problem due to the relatively large number of parameters that are required [103–111]. Other modeling techniques have also been proposed to model multiple-site catalysts [112], but the approach illustrated in Equation 5.12 still remains the most common, likely because of its relative simplicity.

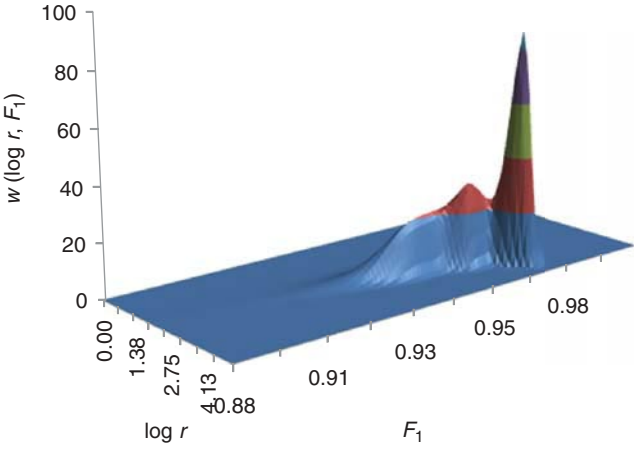

Figure 5.12 Simulated chain length and chemical composition distributions of a polymer made from a three-site catalyst. (*See insert for the color representation of the figure*.)

5.5.2 Particle Breakup, Inter- and Intraparticle Mass and Heat Transfer Resistance Models

With the exception of solution processes, all other commercial olefin polymerization processes use heterogeneous catalysts [53, 54]. When a fresh catalyst particle is introduced in the polymerization reactor (or prepolymerization reactor), monomer molecules diffuse into the catalyst pores and start forming polymer chains. In a properly designed catalyst, the polymer chains fill the pores until the force they exert on the pore walls exceeds their mechanical strength, causing the catalyst particle to break up into smaller fragments. These catalyst fragments are surrounded by entangled growing polymer chains that act as a binder, keeping the fragments together in the expanding polymer/catalyst particle. This particle breakup and exfoliation process is known as the *replication phenomenon* because the polymer particles replicate the shape and size distribution of the catalyst particles.

As usual in heterogeneous catalysis processes [113], inter- and intraparticle mass and heat transfer resistances may develop during polymerization with heterogeneous Ziegler–Natta, Phillips, and supported metallocene catalysts. If significant, the resulting temperature and concentration radial profiles may affect not only the apparent polymerization rate but also the polymer microstructure. The models described in the previous section remain valid, but only locally: slightly different microstructural distributions would be required to describe the polymer made at different radial positions because temperature, monomer/comonomer ratio, and monomer/hydrogen ratio may also be varied. In fact, the original motivation for the development of particle mass and heat transfer models for olefin polymerization was to explain the production of polyolefins with broad MWDs made with heterogeneous Ziegler–Natta catalysts [114]. If significant monomer concentration or temperature profiles occur in the polymer particle, the polymer average molecular weight becomes a function of radial position, broadening the MWD [5].[2]

Several models have been proposed to describe intraparticle heat and mass transfer with heterogeneous coordination catalysts [114], but the most commonly accepted is the multigrain model (MGM) [115–126]. In the MGM, the

[2]Currently, it is accepted that the main reason behind broad MWDs is the presence of more than one type of active site in these catalysts, with mass and heat transfer limitations being a secondary broadening effect of varying importance depending on catalyst type and polymerization conditions.

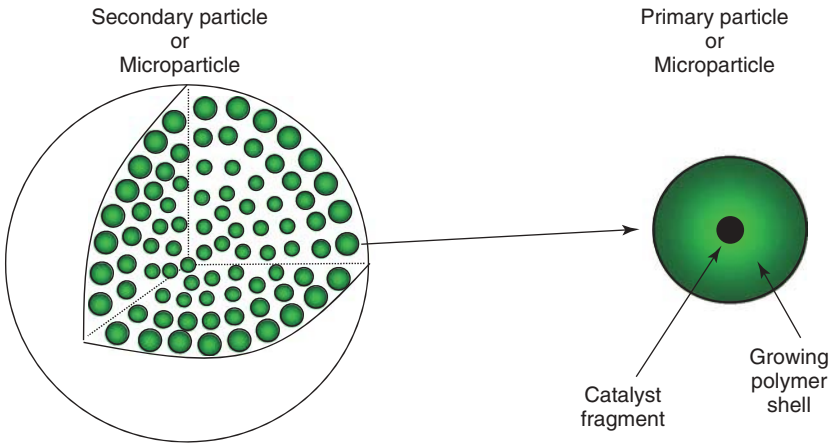

Figure 5.13 The multigrain model (MGM). (*See insert for the color representation of the figure*.)

growing polymer particle (macroparticle or secondary particle) is considered to be composed of several hundreds of catalyst fragments surrounded by growing polymer chains (microparticles or primary particles). Figure 5.13 shows a schematic for the MGM.

Another common single-particle model is the polymeric flow model (PFM), in which a pseudohomogenous hypothesis is made for the macroparticle [127–129]. Instead of being located at the center of microparticles, as in the MGM, active sites are considered to be dispersed in a pseudohomogenous medium with varying radial concentrations. The PFM is somewhat easier to implement than the MGM and leads to similar prediction trends. Several models that combine features of the MGM and PGM have also been developed over the years [114, 130].

The set of equations defining the PGM and MGM are the classic diffusion–reaction equations in spherical coordinates, with and without the pseudohomogenous approximation, respectively, but they must be solved under moving boundary conditions since the particle expands during polymerization; these model equations have been explained in detail in a review dedicated to single-particle models [114].

A few general conclusions have been reached from the extensive use of these single-particle models: (i) intraparticle mass transfer resistances in gas-phase processes are less important than those in slurry processes since gas-phase diffusion coefficients are 2 to 3 orders of magnitude greater than those in slurry; (ii) interparticle heat transfer resistances are more significant in gas-phase processes since gases are poor heat conductors; (iii) heat transfer resistances are greatest in larger catalyst particles because the amount of heat released is proportional to the particle volume, whereas energy removal from the particle is proportional to surface area; (iv) similarly, mass transfer resistances are also more significant in larger catalyst particles since the polymerization rate is proportional to particle volume, while monomer flux to the particle is proportional to surface area; and (v) as the polymer particles grow, both mass and heat transfer limitations decrease, as the number of active sites either remains constant or decreases through deactivation reactions, causing both the heat generation rate and the rate of monomer consumption per unit volume to decrease, while heat and mass flux increase with the expanding surface area.

Figure 5.14 shows how the microstructural distributions developed in the previous section can be used in conjunction with the MGM [131].

The summation of these distributions over the polymer particle, weighted by the amount of polymer made at each radial position, gives the distribution for the whole particle at a given instant in time $w_p(r, y)$,

$$w_p(r, y) = \frac{\int_0^{R_s} R_p(r_s) w(r, y) \mathrm{d}r_s}{\int_0^{R_s} R_p(r_s) \mathrm{d}r_s} \tag{5.13}$$

where $R_p(r_s)$ is the rate of polymerization at a given radial position and R_s is the macroparticle radius. These instantaneous distributions can then be integrated in time to obtain the cumulative distribution in the reactor per polymer particle, $\overline{w}_p(r, y)$,

$$w_p(r, y) = \frac{\int_0^t \int_0^{R_s} R_p(r_s) w(r, y) \mathrm{d}r_s \mathrm{d}t}{\int_0^t \int_0^{R_s} R_p(r_s) \mathrm{d}r_s \mathrm{d}t} \tag{5.14}$$

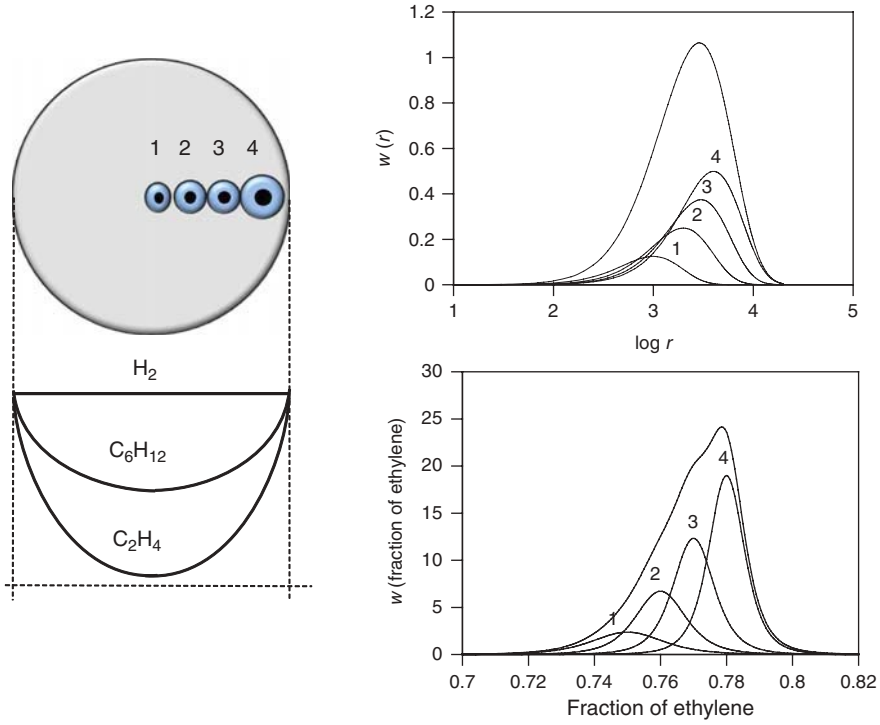

Figure 5.14 Effect of radial concentration profiles on the chain length and chemical composition distributions of an ethylene/1-hexene copolymer (four microparticle layers were used for simplicity sake: many more layers are required in an actual MGM simulation) [131].

A similar approach can be applied for a catalyst containing n site types: the instantaneous CLD and CCD in the particle equal the summation of the distributions over all site types and all radial positions,

$$w_{\mathrm{p}}(r, y) = \frac{\int_0^{R_{\mathrm{s}}} \sum_{j=1}^{n} R_{\mathrm{p},j}(r_{\mathrm{s}}) w_j(r, y) \mathrm{d}r_{\mathrm{s}}}{\int_0^{R_{\mathrm{s}}} \sum_{j=1}^{n} R_{\mathrm{p},j}(r_{\mathrm{s}}) \mathrm{d}r_{\mathrm{s}}} \tag{5.15}$$

Despite being well established, the MGM and PFM can only describe a relatively minor set of phenomena that are important in particle fragmentation and growth. These models usually assume that particle fragmentation is instantaneous and cannot account for a series of important phenomena such as prepolymerization effect, particle agglomeration, fine formation, and reactor fouling, which are issues of significant industrial interest, but difficult to describe even with a semiquantitative mathematical model. Several other models, generally variations of the MGM or PFM, have been developed to try to capture different aspects of particle morphology development during olefin polymerization with heterogeneous catalysts [130, 132–148].

5.5.3 Polymerization Reactor Models

Phenomena taking place from microscale to macroscale influence olefin polymerization rates and polyolefin microstructure. Catalyst type ultimately determines the polymer microstructure for a given set of polymerization conditions such as temperature, monomer/comonomer ratio, and hydrogen concentration, but the polymerization conditions at the active sites are a consequence of the type of catalyst support and reactor used to produce the polyolefin.

A complete phenomenological mathematical model for olefin polymerization in industrial reactors should, in principle, consider phenomena taking place from microscale to macroscale, but this is seldom the case. Most models assume that the conditions in the polymerization reactor are uniform and neglect any mesoscale phenomena, which may be a good approximation for solution polymerization reactors, but may not apply to polymerizations using heterogeneous catalysts.

The reason this relatively weak hypothesis is often made is that the effort required to integrate phenomena taking place from micro- to macroscale in a single model does not necessarily lead to better quantitative predictions when it comes to industrial reactors. Uncertainties in model parameter values, especially for multiple-site catalysts, are

too high to try to decouple the "true" polymerization kinetics from particle mass and heat transfer effects; often apparent kinetic parameters will do an equally good job from an engineering perspective.

Several macroscale models with varying levels of complexity and covering macroscale phenomena such as the reactor residence time effects and micro- and macromixing behavior have been developed for olefin polymerization but is not discussed here in detail for the sake of brevity [149–157].

REFERENCES

1. Boor J. *Ziegler-Natta Catalysts and Polymerizations*. New York: Academic Press, Inc.; 1979.
2. [a] McDaniel Max P. Adv Cat 2010;53:123. [b] Sailors HR, Hogan JP. Polymer News 1981;7:152. [c] Eley DD, Rochester CH, Scurrell MS. Proc Roy Soc Lond A 1972;329:361.
3. [a] Osakada K, Takeuchi D. Adv Polym Sci 2004;171:137. [b] Moore EP Jr,. *Polypropylene Handbook*. Munich, Viena, New York: Hanser Publishers; 1996. p 12.
4. [a] Long WP, Brelow DS. J Am Chem Soc 1960:1953. [b] Halterman RL. Chem Rev 1992;92:965.
5. Sinn H, Kaminsky W. Adv Organomet Chem 1980;18:99.
6. [a] Soga K, Uozumi T, Kaji E. In: Scheirs J, Kaminsky W, editors. *Metallocene-Based Polyolefins*. Chichester: John Wiley and Sons Ltd.; 2000. p I/381. [b] Ewen JA, Jones RL, Razavi A, Ferrara JD. J Am Chem Soc 1988;110:6255. [c] Spaleck W, Küber F, Winter A, Rohrmann J, Bachmann B, Antberg M, Dolle V, Paulus FF. Organometallics 1994;13(3):954. [d] Collins S, Gauthier WJ, Holden DA, Kuntz BA, Taylor NJ, Ward DG. Organometallics 1991;10:2061.
7. [a] Burger P, Debold J, Gutmann S, Hund HU, Brintzinger HH. Organometallics 1992;11:1319. [b] Röll W, Brintzinger HH, Rieger B, Zalk R. Angew Chem Int Ed Engl 1990;29:279.
8. [a] Ewen JA. In: Scheirs J, Kaminsky W, editors. *Metallocene-Based Polyolefins*. Chichester: John Wiley and Sons Ltd.; 2000. p I/3. [b] Ewen JA, Elder MJ, Jones RL, Haspeslagh L, Atwood JL, Bott SG, Robinson K. Makromol Chem Macromol Symp 1991;48/49:253.
9. [a] Soares JBP, McKenna TF, Cheng CP. Coordination polymerization. In: Asua JM, editor. *Polymer Reaction Engineering*. Blackwell Publishing; 2007. p 29–117. [b] Soares JBP. Chem Eng Sci 2001;56:4131. [c] Tomotsu N, Malanga M, Schellenberg J. *Synthesis of syndiotactic polystyrene*. In: Scheirs J, Priddy D, editors. *Modern Styrenic Polymers*. John Wiley and Sons; 2003. p 365. [d] Schellenberg J, Tomotsu N. Prog Polym Sci 2002;27(9):1925.
10. [a] Ishihara N, Seimija T, Kuramoto M, Uoi M. Macromolecules 1986;19:2464. [b] Ishihara N, Kuramoto M, Uoi M. Macromolecules 1988;21:3356.
11. [a] Chum SP, Kao CI, Knight GW. In: Scheirs J, Kaminsky W, editors. *Metallocene-Based Polyolefins*. Chichester: John Wiley and Sons Ltd.; 2000. p I/134, 261. [b] Braunschweig H, Breitling FM. Coord Chem Rev 2006;250(21–22):2691.
12. [a] Pellecchia C, Pappalardo D, D'Arco M, Zambelli A. Macromolecules 1996;29:1158. [b] Lai SY, Wilson JR, Knight GW, Stevens JC, inventors; Dow Chemical Co., assignee. US patent 5, 665, 800. 1997.
13. [a] Kempe R. Chem Eur J 2007;13:2764. [b] Yu Vasil'eva M, Fedorov SP, Nikolaev DA, Oleinik II, Ivanchev SS. Polymer Sci B 2010;52(7–8):443.
14. [a] Kuran W. In: Kuran W, editor. *Principles of Coordination Polymerisation*. John Wiley and Sons Ltd.; 2001. p 275. [b] Burford RP. J Macromol Sci Chem 1982;A17(1):123.
15. Scollard JD, McConville DH, Vittal JJ. Organometallics 1995;14:5478.
16. [a] Beddie C, Wei P, Stephan DW. Can J Chem 2006;84:755. [b] Stephan DW, Guérin F, Spence REH, Koch L, Gao X, Brown SJ, Swabey JW, Wang Q, Xu W, Zoricak P, Harrison DG. Organometallics 1999;18:2046.
17. [a] Kaivalchatchawal P, Suttipitakwong P, Samingprai S, Praserthdam P, Jongsomjit B. Molecules 2011;16:1655. [b] ChunHong W, HuaYi L, YuQi F, YouLiang HU. Chin Sci Bull 2008;53:3164.
18. [a] Capacchione C, Proto A, Ebeling E, Mulhaupt R, Moller K, Spaniol TP, Okuda J. J Am Chem Soc 2003;125:4964. [b] Gibson VC, Spitzmessser SK. Chem Rev 2003;103:283.
19. [a] Scollard JD, McConville DH, Payne NC, Vittal JJ. Macromolecules 1996;29:5241. [b] Liang LCH, Schrock RR, Davis WW, McConville DH. J Am Chem Soc 1999;121:5797. [c] Lee CHH, La Y-H, Park JW. Organometallics 2000;19:344.
20. Mohebbi S, Rayati S. Transit Met Chem 2007;32:1035.
21. Collins S. Coord Chem Rev 2011;255:118.
22. [a] Britovsek GJP, Bruce M, Gibson VC, Kymberly BS, Maddox PJ, Mastroianni S, McTravish SJ, Redshaw C, Solan GA, Strömbergm S, White AJP, Williams DJ. J Am Chem Soc 1999;121:8728. [b] Gibson VC, Redshaw C, Solan GA. Chem Rev 2007;107:1745.
23. [a] Mitani M, Mohri J-I, Yoshida Y, Saito J, Ishii S, Tsuru K, Matsui S, Furuyama R, Nakano T, Tanaka H, Kojoh S-I, Matsugi T, Kashiwa N, Fujita T. J Am Chem Soc 2002;124:3327. [b] Tian J, Hustad D, Coates GW. J Am Chem Soc 2001;123:5134.
24. Friebe PL, Nuyken O, Obrecht W. In: Nuyken O, editor. *Advances in polymer science*. Berlin, Heidelberg: Springer-Verlag; 2006. p 204.
25. Hou Z, Wakatsuki Y. Coord Chem Rev 2002;231:1.
26. Michalak A, Ziegler T. Top Organomet Chem 2005; 12:145.
27. Guan Z, Cotts PM, McCord EF, McLain SJ. Science 1999;283:2059 Available at www.sciencemag.org.
28. [a] Ittel SD, Johnson LK, Brookhart M. Chem Rev 2000;100:1169. [b] Johnson LK, Mecking S, Brookhart M. J Am Chem Soc 1996;118:267.

29. [a] Gibson VC, Redshaw C, Solan GA. Chem Rev 2007;107:1745. [b] Gibson VC. J Chem Soc Chem Comm 1998:849.
30. Wang C, Friedrich S, Younkin TR, Li RT, Grubbs RH, Bransleben DA, Day MW. Organometallics 1998;17:3149.
31. Vandenberg EJ, Repka BC. *Ziegler type polymerizations*. In: Schildknecht C, Skeits I, editors. *Polymerization Processes*. New York: Wiley (Interscience); 1975. p 337.
32. [a] Krauss HL. Proceedings International Congress of Catalysis 5th, 1972, 1973;1:207. [b] Thüne PC, Like R, van Gennip WJH, de Jong AM, Niemantsverdriet JW. J Phys Chem B 2001;105:3073.
33. [a] Pecherskaya YI, Kazanskii VB, Voevodskii VV. Actes Congr Int Catal 2nd 1961 paper 108. [b] Hogan JP. J Polymer Sci A 1970;18:2637.
34. Zheng Z-W, Shi DP, Su PL, Luo ZH, Li XJ. Ind Eng Chem Res 2011;50(1):322.
35. [a] Boor J. *Ziegler-Natta Catalysts and Polymerizations*. New York: Academic Press, Inc.; 1979. p 141. [b] Boor J. *Ziegler-Natta Catalysts and Polymerizations*. New York: Academic Press, Inc.; 1979. p 125.
36. Quirk RP, Kells AM. Polym Int 2000;49:751.
37. [a] EXXON. Jpn patent JP1-503788. 1989; [b] Montagna AA, Floyd JC. MetCon′93; 1993, May 26–28; Houston, TX. Catalyst Consultants Inc., p 171.
38. [a] Rodríguez AS, Kirillov E, Carpentier JF. Coord Chem Rev 2008;252:2115. [b] Knjazhanski SY, Cadenas G, García M, Pérez CM. Organometallics 2002;21:3094.
39. Soares JBP. Chem Eng Sci 2001;56:4131.
40. Cano J, Kunz K. J Organomet Chem 2007;692(21):4411.
41. Makio H, Terao H, Iwashita A, Fujita T. Chem Rev 2011;111(3):2363.
42. Klee JE, Schneider C, Holter D, Burgath A, Frey H, Mulhaupt R. Polymers Adv Tech 2001;12(6):346.
43. [a] Zhang Y, Ning Y, Caporaso L, Cavallo L. J Am Chem Soc 2010;132(8):2695. [b] Talarico G, Cavallo L. Kinet Catal 2006;47(2):289.
44. Kawai K, Fujita T. Topics in organometalic chemistry. In: Zhibin G, editor. *Metal Catalysts in Olefin Polymerization*. Springer; 2009. p 256.
45. Peuckert M, Keim W. J Mol Catal 1984;22(3):289.
46. Nakamura A, Ito S, Nozaki K. Chem Rev 2009;109: 5215.
47. L. Johnson, A. Bennett, P. Butera, K. Dobbs, N. Drysdale, E. Hauptman, A. Ionkin, A. Ittel, E. McCord, S. McLain, C. Radzewich, A. Rinehart, RS. Schiffino, KJ. Sweetman, J. Uradnisheck, L. Wang, Y. Wang and Z. Yin, *Abstracts of Papers, 225th ACS National Meeting*, *New Orleans, LA, United States, March 23–27*, 2003, p. 356, POLY-Publisher: American Chemical Society.
48. Drent E, Dijk RV, Ginkel RV, Oort BV, Pugh RI. Chem Commun 2002:744.
49. Fink G, Steinmetz B, Zechlin J, Przybyla C, Tesche B. Chem Rev 2000;100:1377.
50. [a] Ribeiro MR, Deffieux A, Portela MF. Ind Eng Chem Res 1997;36(4):1224. [b] Y Choi, JBP Soares. Can J Chem Eng 2011, 10.1002/cjce.20583.
51. [a] Arlman EJ. J Catal 1964;3:89. [b] Arlman EJ, Cossee P. J Catal 1964;3:99.
52. Ray WH. Berlin Busengesellschaft fuer Physikalische Chemie 1986;90:947.
53. Soares JBP, McKenna TF, Cheng CP. Coordination polymerization. In: Asua JM, editor. *Polymer Reaction Engineering*. Oxford: Blackwell Publishing; 2007. p 29.
54. Soares JBP, Simon LC. Coordination polymerization. In: Meyer T, Keurentjes J, editors. *Handbook of Polymer Reaction Engineering*. Weinheim: Wiley-VCH; 2005. p 365.
55. Soares JBP. Macromol Mater Eng 2004;289:70.
56. Hamielec AE, MacGregor JF, Penlidis A. Makromol Chem Macromol Symp 1987;10/11:521.
57. Hamielec AE, MacGregor JF, Penlidis A. Copolymerization. In: Allan SG, editor. *Comprehensive Polymer Science*. Oxford: Pergamon Press; 1989. p 17.
58. Xie T, Hamielec AE. Makromol Chem Theory Simul 1993;2:421.
59. Xie T, Hamielec AE. Makromol Chem Theory Simul 1993;2:455.
60. Kissin YV. J Mol Catal 1989;56:220.
61. Kissin YV, Mink RI, Nowlin TE, Brandolini AJ. Top Catal 1999;7:69.
62. Resconi L, Cavallo L, Fait A, Piemontesi F. Chem Rev 2000;100:1253.
63. Garoff T, Johansson S, Pesonen K, Waldvogel P, Lindgren D. Eur Polymer J 2002:121.
64. Kissin YV, Rishina LA, Polym J. J Polymer Sci Chem A 2002;40:1353.
65. Kissin YV, Rishina LA, Polym J. J Polymer Sci Chem A 2002;40:1899.
66. Yestenes M. J Catal 1991;129:383.
67. Wester TS, Ystenes M. Macromol Chem Phys 1997;198: 1623.
68. Shaffer WKA, Ray WH. J Appl Polym Sci 1997;65:1053.
69. Ray WH. J Macromol Sci Rev Macromol Chem 1972;C8:1.
70. Canu P, Ray WH. Comput Chem Eng 1991;15:549.
71. Wulkov M. Macromol Theory Simul 1996;5:393.
72. Wulkov M. Macromol React Eng 2008;2:494.
73. Soares JBP, Hamielec AE. Macromol React Eng 2007;1:53.
74. Soares JBP, Hamielec AE. Macromol React Eng 2008; 2:115.
75. Keii T, Terano M, Kimura K, Ishii K. Makromol Chem Rapid Commun 1987;8:853.
76. Liu B, Matsuoka H, Terano M. Macromol Rapid Commun 2001;22:1.
77. Mori H, Terano M. Trends Polymer Sci 1977;5:314.
78. Di Martino A, Broyer JP, Spitz R, Weickert G, McKenna TF. Macromol Rapid Commun 2005;26:215.
79. Schulz GV. Z Physik Chem 1935;B30:379.

80. Flory PJ. J Am Chem Soc 1877;1936:58.
81. Flory PJ. J Am Chem Soc 1937;59:241.
82. Stockmayer WH. J Chem Phys 1945;13:199.
83. Mayo FR, Lewis FM. J Am Chem Soc 1944;66:1594.
84. Randal JC. *Polymer sequence determination*. In: *Carbon-13 NMR Method*. New York: Academic Press; 1977.
85. Bovey FA, Mirau PA. *NMR of Polymers*. San Diego: Academic Press; 1996.
86. Soares JBP. Macromol Symp 2007;257:1.
87. de Carvalho AB, Gloor PE, Hamielec AE. Polymer 1989;30:280.
88. Rincon-Rubio LM, Wilen CE, Lindfords LE. Eur Polymer J 1990;26:171.
89. Soares JBP, Hamielec AE. Macromol Theory Simul 1996;5:547.
90. Soares JBP, Hamielec AE. Macromol Theory Simul 1997;6:591.
91. Beigzadeh D, Soares JBP, Penlidis A. Polym React Eng 1999;7:195.
92. Simon LC, Soares JBP, de Souza RF. AICHE J 2000;45:1234.
93. Simon LC, Soares JBP, de Souza RF. Chem Eng Sci 2001;56:4181.
94. Simon LC, Soares JBP. Macromol Theory Simul 2002; 11:184.
95. Simon LC, Soares JBP. Ind Eng Chem Res 2005;44:2461.
96. Haag MC, Simon LC, Soares JBP. Macromol Theory Simul 2003;12:142.
97. Gillespie DT. J Phys Chem 1977;81:2340.
98. Soares JBP, Nguyem T. Macromol Symp 2007;260:189.
99. Galvan R, Tirrell M. Chem Eng Sci 1986;41:2385.
100. McAuley KB, MacGregor JF, Hamielec AE. AICHE J 1990;36:837.
101. Soares JBP, Hamielec AE. Polym React Eng 1996;3:261.
102. Soares JBP, Hamielec AE. Macromol Theory Simul 1995;4:305.
103. Vickroy VV, Schneider H, Abbott RF. J Appl Polym Sci 1993;50:551.
104. Soares JBP, Hamielec AE. Polymer 1995;36:2257.
105. Kissin YV, Rishina LA, Vizen EI. J Polymer Sci A: Polymer Chem 2002;40:1899.
106. Kissin YV, Mirabella FM, Meverden CC. J Polym Sci A: Polymer Chem 2005;43:4351.
107. da Silva Filho AA, de Galand GB, Soares JBP. Macromol Chem Phys 2000;201:1226.
108. Sarzotti DM, Soares JBP, Penlidis A. J Polymer Sci, Part B: Polymer Phys 2002;40:2595.
109. Alghyamah AA, Soares JBP. Macromol Rapid Commun 2009;30:384.
110. Soares JBP, Abbott RF, Willis JN, Liu X. Macromol Chem Phys 1996;197:3383.
111. Faldi A, Soares JBP. Polymer 2001;42:3057.
112. Soares JBP. Polym React Eng 1998;6:225.
113. Smith JM. *Chemical Engineering Kinetics*. New York: McGraw-Hill; 1981.
114. McKenna TF, Soares JBP. Chem Eng Sci 2001;56:3931.
115. Crabtree JR, Grimsby FN, Nummelin AJ, Sketchley JM. J Appl Polym Sci 1973;17:959.
116. Nagel EJ, Kirilov VA, Ray WH. Ind Eng Chem Prod Res Dev 1980;19:372.
117. Taylor TW, Choi KY, Yuan H, Ray WH. Physicochemical kinetics of liquid phase propylene polymerization. In: Quirk RP, editor. *Transition Metal Catalyzed Polymerization*. MMI Symposium Series 11. Volume 4. 1981. p 191.
118. Floyd S, Choi KY, Taylor TW, Ray WH. J Appl Polym Sci 1986;32:2935.
119. Floyd S, Choi KY, Taylor TW, Ray WH. J Appl Polym Sci 1986;31:2231.
120. Floyd S, Hutchinson RA, Ray WH. J Appl Polym Sci 1986;32:5451.
121. Hutchinson RA, Chen CM, Ray WH. J Appl Polym Sci 1992;44:1389.
122. Hutchinson RA, Ray WH. J Appl Polym Sci 1987;34:657.
123. Hutchinson RA, Ray WH. J Appl Polym Sci 1990;41:51.
124. Hutchinson RA, Ray WH. J Appl Polym Sci 1991;43:1271.
125. Hutchinson RA, Ray WH. J Appl Polym Sci 1991;43: 1387.
126. Debling JA, Ray WH. Ind Eng Chem Res 1995;34:3466.
127. Schmeal WR, Street JR. AICHE J 1971;17:1189.
128. Schmeal WR, Street JR. J Polymer Sci Polymer Phys 1972;10:2173.
129. Singh D, Merril RP. Macromolecules 1971;4:599.
130. McKenna TFL, Di Martino A, Weickert G, Soares JBP. Macromol React Eng 2010;4:40.
131. Soares JBP, Hamielec AE. Polym React Eng 1995;3:261.
132. Ferrero MA, Chiovetta MG. Polym Eng Sci 1987;27:1436.
133. Ferrero MA, Chiovetta MG. Polym Eng Sci 1987;27:1448.
134. Ferrero MA, Chiovetta MG. Polym Eng Sci 1991;31:886.
135. Ferrero MA, Chiovetta MG. Polym Eng Sci 1991;31:904.
136. Estenoz DA, Chiovetta MG. Polym Eng Sci 1996;36: 2208.
137. Estenoz DA, Chiovetta MG. Polym Eng Sci 1996;36: 2229.
138. Estenoz DA, Chiovetta MG. J Appl Polym Sci 2001; 81:285.
139. Chiovetta MG, Estenoz DA. Macromol Mater Eng 2004;289:1012.
140. Merquior DM, Lima EL, Pinto JC. Polym React Eng 2003;11:133.
141. Merquior DM, Lima EL, Pinto JC. Macromol Mater Eng 2005;290:511.
142. Grof Z, Kosek J, Marek M, Adler PM. AICHE J 2003;49:1002.
143. Kittilsen P, Svendsen HF, McKenna TF. AICHE J 2003;49:1495.

144. Di Martino A, Weickert G, Sidoroff F, McKenna TFL. Macromol React Eng 2007;1:338.
145. Noristi L, Marchetti E, Barruzi G, Sgarzi P. J Polymer Sci A: Polymer Chem 1994;32:3047.
146. Grof Z, Kosek J, Marek M. AICHE J 2048;2005:51.
147. Grof Z, Kosek J, Marek M. Ind Eng Chem Res 2005;44:2389.
148. Horackova B, Grof Z, Kosek J. Chem Eng Sci 2007;62: 5264.
149. Soares JBP, Hamielec AE. Polym React Eng 1996;4:153.
150. Soares JBP, Hamielec AE. Macromol Theory Simul 1995;4:1085.
151. Zacca JJ, Debling JA, Ray WH. Chem Eng Sci 1996;51:4859.
152. Zacca JJ, Debling JA, Ray WH. Chem Eng Sci 1941;1997:52.
153. Zacca JJ, Ray WH. Chem Eng Sci 1993;48:3743.
154. Debling JA, Han GC, Kuipers F, VerBurg J, Zacca JJ, Ray WH. AICHE J 1994;40:506.
155. Debling JA, Zacca JJ, Ray WH. Chem Eng Sci 1969;1997:52.
156. Hatzantonis H, Yiannoulakis H, Yiagopoulos A, Kiparissidis C. Chem Eng Sci 2000;55:3237.
157. Kim JY, Choi KY. Chem Eng Sci 2001;56:4069.